anisms underlying this specificity have not been clear. Our findings indicate that tumstatin is a potent angiogenesis inhibitor because it specifically inhibits protein synthesis in vascular endothelial cells in a αVβ3 integrin–dependent manner, leading to endothelial cell–specific apoptosis.

References and Notes

1. S. McBratney, C. Y. Chen, P. Sarnow, *Curr. Opin. Cell Biol.* **5**, 961 (1993).
2. E. J. Brown, S. L. Schreiber, *Cell* **86**, 517 (1996).
3. S. L. Tan, M. G. Katze, *J. Interferon Cytokine Res.* **19**, 543 (1999).
4. A. C. Gingras, B. Raught, N. Sonenberg, *Genes Dev.* **15**, 807 (2001).
5. Y. Maeshima *et al.*, *J. Biol. Chem.* **275**, 21340 (2000).
6. Y. Maeshima, P. C. Colorado, R. Kalluri, *J. Biol. Chem.* **275**, 23745 (2000).
7. Y. Maeshima *et al.*, *J. Biol. Chem.* **276**, 15240 (2001).
8. Y. Maeshima *et al.*, *J. Biol. Chem.* **276**, 31959 (2001).
9. M. Bushell, L. McKendrick, R. U. Janicke, M. J. Clemens, S. J. Morley, *FEBS Lett.* **451**, 332 (1999).
10. Amino acids 45 to 132 of tumstatin were expressed as recombinant tum-5 in *Escherichia coli* (*7*). Human endostatin was produced in yeast (*15*). We used only soluble protein with a low endotoxin level (less than 50 endotoxin units/mg). T3 peptide (LQRFTTMPFLFCNVNDVCNF), T7 peptide (TMPFLFCNVNDVCNFASRNDYSYWL) consisting of residues 69 to 88 and 74 to 98 of tumstatin, respectively, and mutant T7 peptide (TMPFMFCNINNVCNFASRNDYSYWL) were synthesized as in (*6*, *8*).
11. Supplemental material is available on *Science* Online at www.sciencemag.org/cgi/content/full/295/5552/140/DC1.
12. L. Beretta, A. C. Gingras, Y. V. Svitkin, M. N. Hall, N. Sonenberg, *EMBO J.* **15**, 658 (1996).
13. M. S. O'Reilly *et al.*, *Cell* **88**, 277 (1997).
14. G. Bergers, K. Javaherian, K. M. Lo, J. Folkman, D. Hanahan, *Science* **284**, 808 (1999).
15. M. Dhanabal, R. Volk, R. Ramchandran, M. Simons, V. P. Sukhatme, *Biochem. Biophys. Res. Commun.* **258**, 345 (1999).
16. V. Kumar *et al.*, *J. Biol. Chem.* **275**, 10779 (2000).
17. L. Beretta, Y. V. Svitkin, N. Sonenberg, *J. Virol.* **70**, 8993 (1996).
18. R. J. Jackson, in *Translational Control of Gene Expression*, N. Sonenberg, J. W. B. Hershey, M. B. Mathews, Eds. (Cold Spring Harbor Laboratory Press, Cold Spring Harbor, NY, 2000), p. 127.
19. A. Sudhakar, Y. Maeshima, R. Kalluri, unpublished observations.
20. K. M. Hodivala-Dilke *et al.*, *J. Clin. Invest.* **103**, 229 (1999).
21. J. C. Lively, in preparation.
22. K. Vuori, *J. Membr. Biol.* **165**, 191 (1998).
23. E. Ruoslahti, *Adv. Cancer Res.* **76**, 1 (1999).
24. H. C. Chen, J. L. Guan, *Proc. Natl. Acad. Sci. U.S.A.* **91**, 10148 (1994).
25. F. Vinals, J. C. Chambard, J. Pouyssegur, *J. Biol. Chem.* **274**, 26776(1999).
26. G. J. Brunn *et al.*, *Science* **277**, 99 (1997).
27. A. C. Gingras, B. Raught, N. Sonenberg, *Annu. Rev. Biochem.* **68**, 913 (1999).
28. A. Pause *et al.*, *Nature* **371**, 762 (1994).

29. We thank U. L. Yerramalla for technical assistance and M. Herlyn for the WM-164 melanoma cells. This study was supported in part by NIH grants DK-51711 (R.K.), DK-55001 (R.K.), and PO1-HL66105 (R.O.H.) and research funds from Beth Israel Deaconess Medical Center. Beth Israel Deaconess Medical Center has licensed tumstatin to Ilex Oncology for human clinical trials. R.K. serves as a consultant for Ilex Oncology.

13 August 2001; accepted 9 November 2001

Mediation of Hippocampal Mossy Fiber Long-Term Potentiation by Presynaptic I_h Channels

Jack Mellor, Roger A. Nicoll,* Dietmar Schmitz

Hippocampal mossy fiber long-term potentiation (LTP) is expressed presynaptically, but the exact mechanisms remain unknown. Here, we demonstrate the involvement of the hyperpolarization-activated cation channel (I_h) in the expression of mossy fiber LTP. Established LTP was blocked and reversed by I_h channel antagonists. Whole-cell recording from granule cells revealed that repetitive stimulation causes a calcium- and I_h-dependent long-lasting depolarization mediated by protein kinase A. Depolarization at the terminals would be expected to enhance transmitter release, whereas somatic depolarization would enhance the responsiveness of granule cells to afferent input. Thus, I_h channels play an important role in the long-lasting control of transmitter release and neuronal excitability.

A remarkable property of many excitatory synapses in the central nervous system is their ability to undergo activity-dependent, long-lasting increases in synaptic strength, referred to as LTP, a process that may underlie certain forms of memory. In most cases LTP requires the activation of postsynaptic *N*-methyl-D-aspartate (NMDA) receptors (*1*, *2*). However, LTP at hippocampal mossy fiber synapses is independent of NMDA receptor activation (*3*, *4*) and is proposed to be initiated by a rise in presynaptic calcium (*4*–*6*) [but see (*7*)], which results in a persistent increase in the probability of transmitter release (*8*, *9*). The mechanism involved in the persistent increase in evoked release is not clear, but considerable evidence supports a role for adenosine 3′,5′-monophosphate (cAMP) (*10*–*13*). In addition, genetic deletion of the synaptic vesicle–associated proteins Rab3A or RIM (which binds to Rab3A) also abolishes mossy fiber LTP (*14*, *15*). Recent results have shown that the presynaptic facilitation of synaptic transmission at the crustacean neuromuscular junction by cAMP involves I_h channels (*16*). Because cAMP is proposed to play a role in mossy fiber LTP, we examined a possible role for I_h in this form of plasticity.

Throughout this study we used the specific I_h channel blocker ZD7288 to examine the role of I_h (*17*). We compared the magnitude of mossy fiber LTP in control slices to that obtained in slices incubated in 1 μM ZD7288 (*18*). Tetanization of the mossy fibers in ZD7288 caused a transient posttetanic potentiation that decayed over a 10-min period toward control values (110 ± 11%, 25 to 30 min, $n = 6$). In contrast, in control slices tetanization caused a 192 ± 7% ($n = 9$) potentiation (Fig. 1A). Elevating cAMP causes a large enhancement in mossy fiber synaptic transmission that occludes LTP (*10*, *11*). In the present experiments, the adenylyl cyclase activator forskolin (50 μM, 5 min) caused a large enhancement in control conditions (275 ± 36%, 25 to 30 min, $n = 14$). This enhancement was strongly reduced by prior incubation of the slices in ZD7288 (135 ± 9%, $n = 6$) (Fig. 1B).

Blockade of both LTP and the cAMP-mediated enhancement by ZD7288 suggests that I_h channels are involved downstream of both tetanus and cAMP elevation and could perhaps be important for the maintenance of synaptic enhancement. ZD7288 was thus applied after the tetanus or application of forskolin. Because of the slow onset of action of 1 μM ZD7288, we increased the concentration to 50 μM (*19*). We performed three types of interleaved experiments: ZD7288 alone, LTP alone, and ZD7288 applied after the induction of LTP. These three sets of experiments are superimposed in Fig. 2A. ZD7288 reversed LTP over a period of 20 to 30 min. The decrease in paired pulse facilitation associated with LTP was also reversed (control, 81 ± 4%; ZD7288, 104 ± 6%). To confirm that ZD7288 reverses established LTP, we made recordings from two independent mossy fiber inputs so that we could simultaneously record the effects of ZD7288 on baseline responses and LTP (Fig. 2B). Again, ZD7288 completely reversed LTP. The fors-

Departments of Cellular and Molecular Pharmacology and Physiology, University of California, San Francisco, CA 94143, USA.

*To whom correspondence should be addressed. E-mail: nicoll@phy.ucsf.edu

kolin-induced enhancement was also reversed when ZD7288 was applied after the enhancement had developed (Fig. 2C).

ZD7288 is a specific blocker of I_h channels, with no reported nonspecific effects at concentrations in excess of 50 μM (*17*). Nonetheless, we considered other agents that are reported to block I_h. Extracellular Cs^+ (1 mM) blocks I_h, but this concentration also blocks inward rectifier potassium channels and produced an enhancement in mossy fiber transmission (*20*). We thus used another organic I_h channel blocker, DK-AH269, which acts in a mechanistically distinct but less specific manner with respect to ZD7288 (*17, 21, 22*). Application of DK-AH269 (100 μM) caused a similar reversal of LTP (Fig. 2D), thus confirming that ZD7288 is acting specifically on I_h channels.

How might I_h exert its presynaptic effects? In many cells I_h contributes to the resting membrane potential and a rise in cAMP enhances I_h, resulting in a depolarization (*21*). We have previously shown that modest depolarization of mossy fibers by application of potassium enhances synaptic transmission (*23*) and that this is associated with a decrease in the fiber volley latency (the latency between the stimulus artifact and the midpoint of the fiber volley) (*24, 25*). We therefore examined the fiber volley latency during LTP and the application of forskolin. During the tetanus and immediately afterward there is an increase in the latency, which then switches into a long-lasting decrease; this persistent decrease in latency is blocked by ZD7288 (Fig. 3A). Forskolin, but not the inactive analog dideoxyforskolin, also caused a ZD7288-sensitive decrease in fiber volley latency (92 ± 21 μs, n = 10) (Fig. 3B), and this effect was largely blocked by the protein kinase A (PKA) inhibitor H-89 (10 μM) (increase of 21 ± 14 μs, n = 4, $P < 0.05$). A reduction in fiber volley latency of similar magnitude was caused by the addition of 4 mM potassium (Fig. 3C). These findings are consistent with a scenario where a presynaptic rise in calcium activates the calcium/calmodulin–sensitive adenylyl cyclase I (AC I), which (via cAMP) enhances I_h, resulting in a depolarization of the mossy fiber and enhanced release of glutamate.

To examine this model, we made recordings from dentate granule cells, which give rise to the mossy fibers and contain high levels of AC I (*26–28*). The granule cell body was also extremely sensitive to changes in potassium. Application of 4 mM potassium, which mimics the decrease in fiber volley latency associated with mossy fiber LTP and the action of forskolin (Fig. 3C), causes a 10.7 ± 1.0 mV (n = 10) depolarization of the granule cell (Fig. 3, D and E) and an increase in the granule cell somatic action potential half-width from 0.85 ± 0.01 ms to 1.04 ± 0.01 ms (n = 4). This sensitivity to potassium is presumably related to the very negative resting membrane potential of granule cells [~ −84 mV, present study and (*29*)] relative to CA3 and CA1 pyramidal cells, and is similar to the membrane potential recorded from mossy fiber boutons (*30*). CA3 pyramidal cells were much less sensitive to changes in potassium (Fig. 3E).

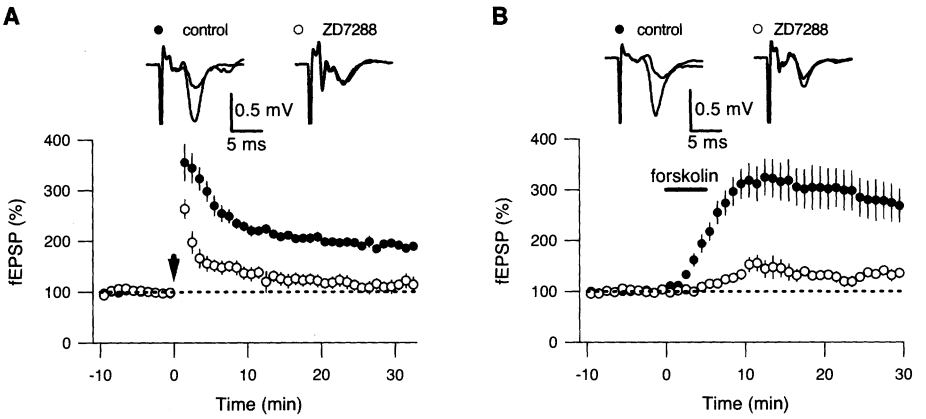

Fig. 1. ZD7288 blocks mossy fiber LTP and cAMP-mediated enhancement. **(A)** Tetanic stimulation (arrow) of mossy fibers produces robust LTP in control conditions, which is greatly reduced by incubating slices in ZD7288 (1 μM) for at least 2 hours before and then during the experiment. Sample traces from two experiments taken during baseline and 30 min after tetanus are shown above. **(B)** Forskolin application (50 μM, 5 min) produces a large enhancement in control conditions, which is severely reduced by prior incubation with ZD7288 (1 μM). Sample traces from two experiments are shown above.

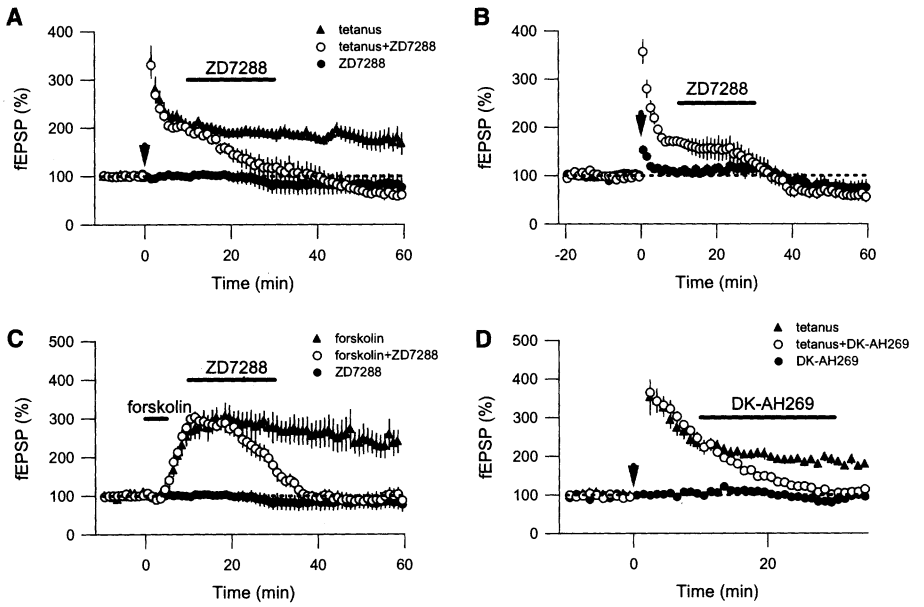

Fig. 2. I_h channels are required in the maintenance of LTP and forskolin enhancement. **(A)** Application of ZD7288 (50 μM) 10 min after the tetanus (arrow) reverses mossy fiber LTP (77 ± 10%, 50 to 60 min and after correcting for baseline depression, n = 7). Application of ZD7288 to interleaved slices reduces the baseline to 83 ± 17% (50 to 60 min, n = 7). **(B)** Two mossy fiber inputs were simultaneously recorded and LTP was induced in one pathway. Application of ZD7288 after the induction of LTP reverses the enhancement (89 ± 14%, 50 to 60 min and after correcting for baseline depression, n = 7). **(C)** Application of ZD7288 10 min after the forskolin application reverses the enhancement (107 ± 23%, 50 to 60 min and after correcting for baseline depression, n = 5). All experiments in (A) to (C) were performed in the presence of the $GABA_B$ antagonist SCH50911 (20 μM) with raised divalent concentrations (4 mM each). **(D)** Application of DK-AH269 (100 μM, 20 min) 10 min after the tetanus also reverses LTP (110 ± 7%, 30 to 35 min, n = 6) but has little effect on the baseline responses (96 ± 8%, n = 6).

Both CA3 and CA1 pyramidal cells express functional I_h channels (*31*), but expression data and electrophysiological recordings show relatively weak expression of I_h channels in dentate granule cells (*29, 31–33*). We therefore used perforated patch recording to test for the presence of I_h currents in these cells. Hyperpolarizing steps from −50 mV produced time-dependent inward currents

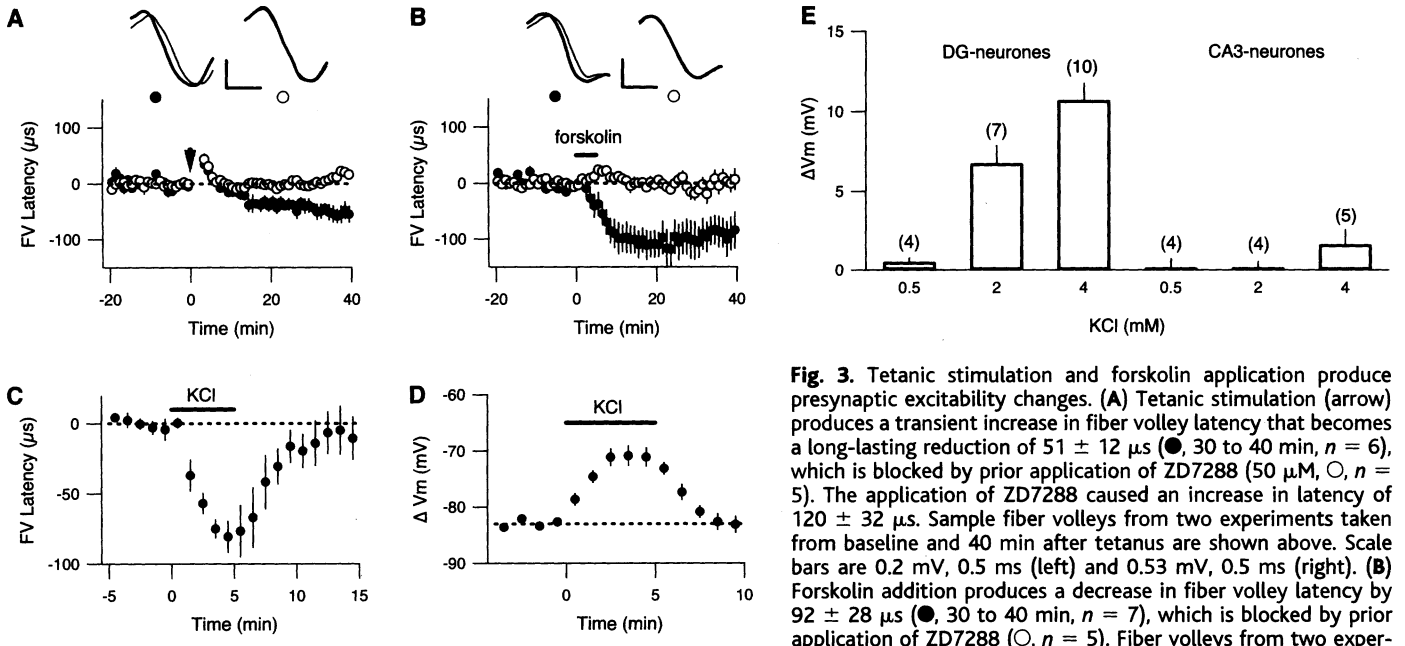

Fig. 3. Tetanic stimulation and forskolin application produce presynaptic excitability changes. (**A**) Tetanic stimulation (arrow) produces a transient increase in fiber volley latency that becomes a long-lasting reduction of 51 ± 12 μs (●, 30 to 40 min, n = 6), which is blocked by prior application of ZD7288 (50 μM, ○, n = 5). The application of ZD7288 caused an increase in latency of 120 ± 32 μs. Sample fiber volleys from two experiments taken from baseline and 40 min after tetanus are shown above. Scale bars are 0.2 mV, 0.5 ms (left) and 0.53 mV, 0.5 ms (right). (**B**) Forskolin addition produces a decrease in fiber volley latency by 92 ± 28 μs (●, 30 to 40 min, n = 7), which is blocked by prior application of ZD7288 (○, n = 5). Fiber volleys from two experiments are shown above. Scale bars are 0.15 mV, 0.5 ms (left) and 0.23 mV, 0.5 ms (right). (**C**) Bath application of KCl (4 mM, 5 min) produces a reversible decrease in fiber volley latency of 81 ± 11 μs (n = 5). (**D**) Whole-cell recordings from granule cell in current-clamp mode showed a reversible depolarization with KCl application (4 mM, n = 4). (**E**) A comparison of the effects of KCl on the membrane potential of granule cells and CA3 pyramidal cells (n values are given in parentheses).

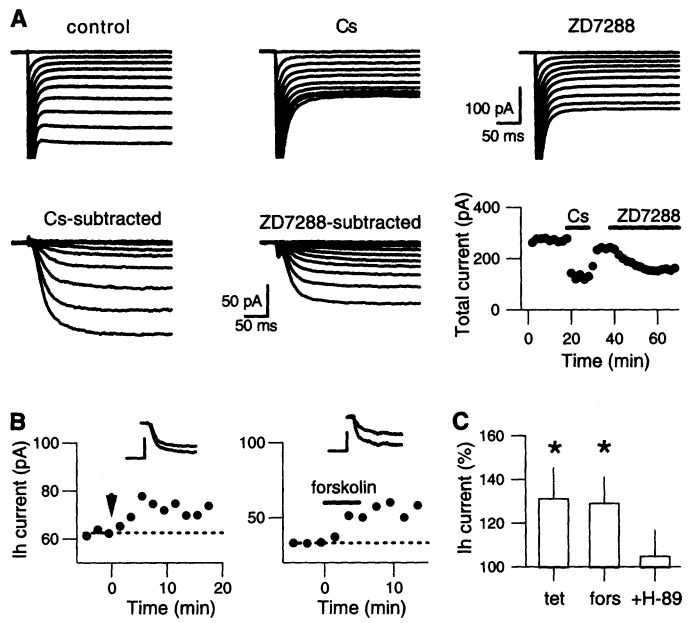

Fig. 4. I_h currents from granule cells are modulated by tetanic stimulation or forskolin addition. (**A**) Voltage steps from −50 mV to −140 mV in 10-mV steps produce inward currents in granule cells held under the perforated patch configuration, which are partially blocked by CsCl (1 mM) and ZD7288 (50 μM). Sample traces show currents under three conditions (top) and subtracted slowly activating I_h currents (bottom, τ = 27 ms for step from −50 mV to −140 mV from ZD7288 subtraction). The graph shows the time course of the experiment. In all granule cells tested, the average activation time constant was 30 ± 7 ms and the average I_h-mediated current, determined by Cs subtraction, was 99 ± 26 pA (n = 7). Average input resistance was 693 ± 89 megohms. (**B**) Individual experiments showing the time course of I_h current (voltage steps from −50 mV to −120 mV measured by Cs subtraction) modulation by tetanus (arrow) or forskolin addition. Sample traces show Cs-subtracted I_h currents before and 10 min after tetanus (scale bars, 50 pA, 100 ms) and forskolin addition (scale bars, 35 pA, 100 ms). (**C**) Average I_h current enhancement by tetanic stimulation, forskolin addition, or forskolin addition after H-89 incubation (n = 8, n = 5, and n = 5, respectively; $^*P < 0.05$). Access and input resistances were continuously monitored, and cells were discarded if these values did not remain constant during the experiment.

that were reduced by CsCl (1 mM) and ZD7288 (50 μM) (Fig. 4A). Subtraction of the current remaining after either CsCl or ZD7288 application from the control current revealed the slowly activating I_h-mediated current (Fig. 4A). Current-voltage plots revealed that I_h begins to activate at ~ −60 mV (*34*). I_h currents with similar characteristics have been found in the presynaptic terminals of cerebellar basket cells (*35*).

Interestingly, firing action potentials in the granule cell at 25 Hz for 5 s with depolarizing current pulses increased the size of I_h, as did the application of forskolin (Fig. 4, B and C). The forskolin-induced I_h enhancement was attenuated by preincubation of slices in H-89 (Fig. 4C). This finding leads to a number of predictions concerning the activity-dependent control of the granule cell membrane potential. Repetitive activation of granule cells resulted in a long-lasting membrane depolarization, which was absent in the presence of ZD7288 (Fig. 5, A and B). In contrast, an identical repetitive activation of CA3 pyramidal cells had no effect on the membrane potential (Fig. 5C). Previous studies have shown that mossy fiber LTP is dependent on the presence of extracellular calcium (*5*). Similarly, repetitive activation of granule cells in the absence of extracellular calcium failed to depolarize the cells, but introduction of calcium into the bathing solution restored the tetanus-induced depolarization (Fig. 5D). Forskolin also caused a ZD7288-sensitive depolarization of granule cells (Fig. 5E). The tetanus-induced depolarization not only required the presence of calcium, but also, similar to mossy fiber LTP (*10, 11*), required PKA activation because it was strongly inhibited in the presence of the PKA inhibitor H-89 (Fig. 5F). Likewise, the forskolin-induced depolarization was also inhibited by H-89 (Fig. 5G).

cAMP directly modulates I_h channels by shifting the voltage dependence of activation to depolarized potentials (*21*), but the degree of enhancement varies markedly depending

on the I_h channel subtype (*36, 37*). It has also been reported that PKA can enhance I_h (*38*). Furthermore, inhibitors of PKA can, in some instances, block the cAMP-induced enhancement (*38, 39*) and phosphatase inhibitors can increase I_h conductance (*40*). Given that the effects that we observe develop slowly over a number of minutes, and given that the effect of forskolin on the fiber volley latency and the tetanus-induced depolarization of granule cells is strongly inhibited by the PKA inhibitor H-89, we favor the view that the membrane effects we observe are due primarily to the action of PKA on I_h. The involvement of PKA in these effects is also consistent with the finding that PKA blockade (*10, 11*) or genetic deletion (*13*) inhibits mossy fiber LTP. Our results do not exclude a contribution of a direct action of cAMP on I_h, nor do they exclude a contribution of the well-established direct actions of cAMP and PKA on the transmitter release machinery (*41–43*). Finally, although we favor the idea that the action of I_h on transmitter release results from membrane depolarization, we cannot exclude a more direct action of I_h on transmitter release, as has been proposed at the crayfish neuromuscular junction (*16, 44*).

Previous data showing that mossy fiber LTP, but not cAMP-mediated enhancement, is blocked in Rab3A or RIM knockout mice (*14, 15*) implies that LTP and cAMP enhancement are not synonymous. However, the observation that ZD7288 blocks both LTP and cAMP-mediated enhancement suggests that both phenomena share a common expression locus: the I_h channel. Such a conclusion is consistent with earlier results demonstrating the occlusion of LTP by forskolin and vice versa (*10, 11*). Hence, Rab3A and RIM may be upstream of cAMP in the LTP induction pathway, whereas I_h channels are downstream.

Our results on mossy fiber synapses and the granule cell soma lead to a simple model for the induction and expression of mossy fiber LTP. We propose that calcium entry into the presynaptic terminal (as well as the granule cell soma and dendrites) during repetitive stimulation activates the calcium-calmodulin–sensitive AC I. The rise in cAMP activates PKA, which enhances I_h, resulting in a depolarization. We previously found that potassium-induced depolarization can enhance mossy fiber transmission (*23*). This could occur by a mechanism in which the depolarization causes a broadening of the action potential by slowing spike repolarization. Indeed, such spike broadening was observed with our granule cell recordings (Fig. 5A); moreover, recordings from mossy fiber boutons show that evoked calcium entry and synaptic release are exquisitely sensitive to action potential width (*30*). However, our results do not rule out a mechanism whereby the depolarization causes a tonic activation of voltage-dependent calcium channels (*45*). It should also be mentioned that mossy fibers form synapses on a number of other cell types, none of which show the same form of LTP as that described here (*46*). It will be interesting to determine why only certain synaptic release sites are sensitive to membrane potential changes.

Our granule cell recordings shed light on the possible mechanisms underlying mossy fiber LTP, but more provocatively, they also demonstrate an activity-dependent process that involves the soma/dendritic compartment of the cell as well as its terminal. Central to this global change in excitability is the finding that AC I appears to be distributed throughout the granule cell (*26–28*). As a result, granule cell activity not only causes a long-lasting increase in transmitter release, but also a long-lasting increase in the responsiveness of granule cells to afferent synaptic input. These findings have implications for the flow of information through the dentate gyrus and for models of epilepsy involving this area of the brain.

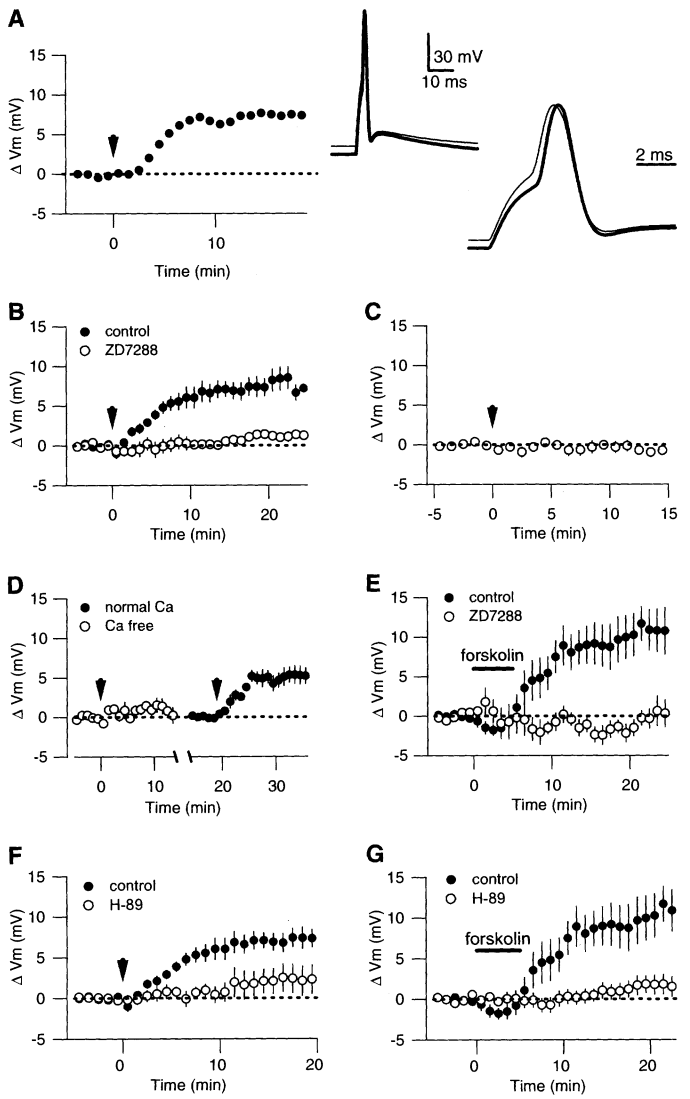

Fig. 5. Long-term depolarization of granule cells by tetanus or forskolin is mediated by PKA and I_h channels. **(A)** Example experiment showing depolarization after tetanic stimulation (left) and the resultant broadening of the action potential (right). Each set of example traces shows the same data taken during baseline and 10 min after tetanus but on different horizontal scales. **(B)** Tetanic stimulation (arrow) of granule cells held under perforated patch conditions causes a slowly developing depolarization of 6.8 ± 1.1 mV (20 to 25 min, n = 13), which is blocked by prior incubation with ZD7288 for at least 30 min (10 μM, n = 9). **(C)** CA3 pyramidal cells show no activity-dependent depolarization. **(D)** Activity-dependent long-term depolarization is dependent on extracellular calcium. Tetanization of granule cells in nominally calcium-free solution failed to evoke a depolarization. However, a depolarization in the same cells was evoked after switching to normal calcium (n = 7). **(E)** Forskolin also causes a long-term depolarization of granule cells (9.2 ± 2.8 mV, n = 7), which is blocked by prior incubation in ZD7288 (n = 5). The specific PKA inhibitor H-89 (slices incubated in 10 μM for at least 4 hours and maintained in H-89 during the experiment) reduces activity-dependent **(F)** and forskolin-induced **(G)** long-term depolarization (n = 7 and 9, respectively). Control data are the same as in (B) and (E).

References and Notes

1. T. V. Bliss, G. L. Collingridge, *Nature* **361**, 31 (1993).
2. R. C. Malenka, R. A. Nicoll, *Science* **285**, 1870 (1999).
3. E. W. Harris, C. W. Cotman, *Neurosci. Lett.* **70**, 132 (1986).
4. R. A. Zalutsky, R. A. Nicoll, *Science* **248**, 1619 (1990).
5. P. E. Castillo, M. G. Weisskopf, R. A. Nicoll, *Neuron* **12**, 261 (1994).
6. J. Mellor, R. A. Nicoll, *Nature Neurosci.* **4**, 125 (2001).
7. M. F. Yeckel, A. Kapur, D. Johnston, *Nature Neurosci.* **2**, 625 (1999).
8. R. A. Nicoll, R. C. Malenka, *Nature* **377**, 115 (1995).
9. D. A. Henze, N. N. Urban, G. Barrionuevo, *Neuroscience* **98**, 407 (2000).
10. M. G. Weisskopf, P. E. Castillo, R. A. Zalutsky, R. A. Nicoll, *Science* **265**, 1878 (1994).
11. Y. Y. Huang, X. C. Li, E. R. Kandel, *Cell* **79**, 69 (1994).

12. E. C. Villacres, S. T. Wong, C. Chavkin, D. R. Storm, *J. Neurosci.* **18**, 3186 (1998).
13. Y. Y. Huang *et al.*, *Cell* **83**, 1211 (1995).
14. P. E. Castillo *et al.*, *Nature* **388**, 590 (1997).
15. P. E. Castillo, S. Schoch, R. C. Malenka, T. C. Südhof, *Soc. Neurosci. Abstr.* **27**, Program 6.12 (2000).
16. V. Beaumont, R. S. Zucker, *Nature Neurosci.* **3**, 133 (2000).
17. N. C. Harris, A. Constanti, *J. Neurophysiol.* **74**, 2366 (1995).
18. Transverse slices of hippocampi from Sprague-Dawley rats (18 to 30 days old) were obtained using standard methods (*30*). Slices were initially maintained in artificial cerebrospinal fluid (ACSF) containing a high concentration of sucrose: 87 mM NaCl, 26 mM $NaHCO_3$, 10 mM glucose, 75 mM sucrose, 2.5 mM KCl, 0.5 mM $CaCl_2$, 7 mM $MgSO_4$, and 1 mM NaH_2PO_4. This medium was ice-cold for cutting, warmed to 35°C for 30 min immediately after, and then cooled to room temperature for a further 30 min. The ACSF was then switched to one that contained 119 mM NaCl, 26 mM $NaHCO_3$, 10 mM glucose, 2.5 mM KCl, 2.5 mM $CaCl_2$, 1.3 mM $MgSO_4$, and 1 mM NaH_2PO_4. All ACSF was equilibrated with 95% O_2 and 5% CO_2. The slices were then transferred to the experimental chamber, mounted on an upright microscope, where they were continuously superfused with normal ACSF (2 to 3.5 ml/min) at room temperature. Field excitatory postsynaptic potentials (fEPSPs) were recorded with extracellular electrodes filled with 1 M NaCl (2 to 4 megohms). D-2-Amino-5-phosphonovaleric acid (10 μM) was present throughout all LTP experiments. To elicit mossy fiber responses, we placed bipolar tungsten electrodes in the granule cell layer of the dentate gyrus. Frequency of stimulation was 0.05 Hz. Tetanic stimulation was 125 pulses, 25 Hz throughout the study. The group II metabotropic glutamate receptor agonist DCG-IV (1 to 2 μM) was applied at the end of each experiment to verify that the signal was generated by mossy fiber synapses. Patch-clamp recordings from CA3 pyramidal and dentate granule cells were obtained with either the whole-cell or perforated patch configuration. Cells were visualized using Nomarski-type differential interference contrast imaging with infrared illumination. The pipette solution (pH 7.4, 280 mOsm) contained 130 mM K-gluconate, 5 mM KCl, 10 mM Hepes, 1 mM $MgCl_2$, and 0.3 mM Na_2–adenosine triphosphate. For perforated patch recording, the tip was filled with a solution containing 120 mM KCl, 8 mM NaCl, 10 mM Hepes, 5 mM $CaCl_2$, 3 mM $MgCl_2$, and 5 mM QX-314Cl (RBI). The pipette was backfilled with this solution supplemented with amphotericin B (0.6 mg/ml). For perforated patch recordings, seals were attained in external solution that was nominally Ca-free. Borosilicate glass pipettes were pulled to tip resistances between 2 and 10 megohms. Access resistances were continuously monitored. Data were collected and analyzed using Igor Pro software. Synaptic responses were filtered at 2 to 20 kHz and digitized at 20 to 100 kHz. DK-AH269 was a gift from Boehringer Ingelheim. All measurements are given as means ± SE. Statistical significance was tested with Student's *t* test.
19. ZD7288 (50 μM) applied for 20 min caused a modest but consistent and stable reduction in synaptic transmission as measured by field potentials (~30%). This effect appeared to be due to a presynaptic action, because (i) a similar reduction of α-amino-3-hydroxy-5-methyl-4-isoxazolepropionic acid (AMPA)–mediated excitatory postsynaptic currents was seen with whole-cell recording in which postsynaptic I_h was blocked by intracellular application of QX-314Cl (64 ± 9%, n = 7), (ii) the NMDA-mediated excitatory postsynaptic currents were similarly depressed (55 ± 14%, n = 3), and (iii) ZD7288 caused a small but significant increase in paired pulse facilitation (118 ± 5%, n = 6, $P < 0.05$), which correlates with a decrease in presynaptic release.
20. CsCl (1 mM) produced a >300% increase in fEPSP amplitude (n = 6). Once stability had been reached after ~60 min, tetanic stimulation or forskolin addition failed to further enhance the fEPSP (n = 3 each). Given the direct effect of Cs on the fEPSP, presumably unrelated to I_h, this blockade is difficult to interpret.
21. H. C. Pape, *Annu. Rev. Physiol.* **58**, 299 (1996).
22. D. Janigro, M. E. Martenson, T. K. Baumann, *J. Membr. Biol.* **160**, 101 (1997).
23. D. Schmitz, J. Mellor, R. A. Nicoll, *Science* **291**, 1972 (2001).
24. J. D. Kocsis, R. C. Malenka, S. G. Waxman, *J. Physiol.* **334**, 225 (1983).
25. D. Schmitz, M. Frerking, R. A. Nicoll, *Neuron* **27**, 327 (2000).
26. P. F. Worley, J. M. Baraban, E. B. De Souza, S. H. Snyder, *Proc. Natl. Acad. Sci. U.S.A.* **83**, 4053 (1986).
27. Z. G. Xia, C. D. Refsdal, K. M. Merchant, D. M. Dorsa, D. R. Storm, *Neuron* **6**, 431 (1991).
28. C. E. Glatt, S. H. Snyder, *Nature* **361**, 536 (1993).
29. K. J. Staley, T. S. Otis, I. Mody, *J. Neurophysiol.* **67**, 1346 (1992).
30. J. R. P. Geiger, P. Jonas, *Neuron* **28**, 927 (2000).
31. B. Santoro *et al.*, *J. Neurosci.* **20**, 5264 (2000).
32. S. Moosmang, M. Biel, F. Hofmann, A. Ludwig, *Biol. Chem.* **380**, 975 (1999).
33. J. Stabel, E. Ficker, U. Heinemann, *Neurosci. Lett.* **135**, 231 (1992).
34. J. Mellor, R. A. Nicoll, D. Schmitz, data not shown.
35. A. P. Southan, N. P. Morris, G. J. Stephens, B. Robertson, *J. Physiol.* **526**, 91 (2000).
36. M. Biel, A. Ludwig, X. Zong, F. Hofmann, *Rev. Physiol. Biochem. Pharm.* **136**, 165 (1999).
37. B. J. Wainger, M. DeGennaro, B. Santoro, S. A. Siegelbaum, G. R. Tibbs, *Nature* **411**, 805 (2001).
38. N. Abi-Gerges *et al.*, *J. Physiol.* **523**, 377 (2000).
39. F. Chang, I. S. Cohen, D. DiFrancesco, M. R. Rosen, C. Tromba, *J. Physiol.* **440**, 367 (1991).
40. E. A. Accili, G. Redaelli, D. DiFrancesco, *J. Physiol.* **500**, 643 (1997).
41. L. E. Trudeau, D. G. Emery, P. G. Haydon, *Neuron* **17**, 789 (1996).
42. T. Sakaba, E. Neher, *Proc. Natl. Acad. Sci. U.S.A.* **98**, 331 (2001).
43. C. Chen, W. G. Regehr, *J. Neurosci.* **17**, 8687 (1997).
44. R. C. Froemke, V. Beaumont, R. S. Zucker, *Soc. Neurosci. Abstr.* **27**, Program 612.6 (2000).
45. R. Turecek, L. O. Trussell, *Nature* **411**, 587 (2001).
46. K. Toth, G. Suares, J. J. Lawrence, E. Philips-Tansey, C. J. McBain, *J. Neurosci.* **20**, 8279 (2000).
47. We thank members of the Nicoll lab for useful comments and discussion. Supported by a Wellcome Trust Travelling Fellowship (J.M.) and by a grant from the Deutsche Forschungsgemeinschaft (Emmy-Noether-Programm) (D.S.). R.A.N. is a member of the Keck Center for Integrative Neuroscience and the Silvio Conte Center for Neuroscience Research and is supported by grants from NIH and the Bristol-Myers Squibb Co.

11 July 2001; accepted 12 November 2001

Sitosterol-β-glucoside as Primer for Cellulose Synthesis in Plants

Liangcai Peng,* Yasushi Kawagoe,† Pat Hogan, Deborah Delmer‡

Cellulose synthesis in plants requires β-1,4-glucan chain initiation, elongation, and termination. The process of chain elongation is likely to be distinct from the process of chain initiation. We demonstrate that a CesA glucosyltransferase initiates glucan polymerization by using sitosterol-β-glucoside (SG) as primer. Cotton fiber membranes synthesize sitosterol-cellodextrins (SCDs) from SG and uridine 5′-diphosphate–glucose (UDP-Glc) under conditions that also favor cellulose synthesis. The cellulase encoded by the *Korrigan* (*Kor*) gene, required for cellulose synthesis in plants, may function to cleave SG from the growing polymer chain.

Cellulose (β-1,4-glucan) microfibrils provide strength and flexibility to plant tissues and are also of great importance to wood, paper, textile, and chemical industries. Genetic evidence implicates plant *CesA* genes, homologous to bacterial cellulose synthases, and the *Korrigan* (*Kor*) gene, a membrane-associated cellulase, in cellulose synthesis (*1–5*).

Herbicides that disrupt cellulose synthesis include 2,6-dichlorobenzonitrile (DCB), which acts in a way that is not understood (*6*), and isoxaben, which may interact directly or indirectly with certain CesA proteins (*7*). Another herbicide, thiatriazene-based CGA 325'625, inhibits synthesis of crystalline cellulose and causes accumulation of a noncrystalline cellulose, which, upon treatment with cellulase, releases CesA protein (*8*) and a small amount of sitosterol linked to glucose (*9*). Because hydrophobic glycosides can function as primers for other glycosyltransferases (*10–14*), sitosterol-glucoside (SG) may serve as a primer for glucan chain elongation, an idea supported by observations that it is synthesized on the inner face of plant plasma membranes (*15*), where cellulose synthesis occurs. An enzyme, UDP-Glc:sterol glucosyltransferase (SGT), which is responsible for synthesis of sterol-β-glucosides, has been found associated with plasma membranes in various plants, including cotton fibers (*16*). Diglucosyl and triglucosylsterols of unknown function have also been isolated from rice bran (*17*).

When cotton fiber membranes are incubated with ^{14}C-labeled UDP-Glc in Tris buffer (*18*), two major compounds soluble in chloroform:methanol (C:M) are synthesized that migrate on thin-layer chromatography (TLC) as SG and SG acylated with palmitic acid (ASG) (Fig. 1A, lane 1). The glucose is in terminal linkage to sterol, >95% of which is sitosterol (*19*). Replacing Tris with Mops

Section of Plant Biology, University of California Davis, One Shields Avenue, Davis, CA 95616, USA.

*Present address: Plant Gene Expression Center, 800 Buchanan Street, Albany CA 94710–1198, USA.
†Present address: National Institute of Agrobiological Resources, Kannondai 2-1-2, Tsukuba, Ibaraki, Japan 305-8602.
‡To whom correspondence should be addressed: E-mail: dpdelmer@ucdavis.edu